Determination of the Global Secondary Structure of Proteins by Furier Transform Infrared (FTIR) Spectroscopy

ARTICLE *in* TRENDS IN FOOD SCIENCE & TECHNOLOGY · JUNE 1993

Impact Factor: 4.65 · DOI: 10.1016/0924-2244(93)90119-U

Review

Determination of the global secondary structure of proteins by Fourier transform infrared (FTIR) spectroscopy

Thomas F. Kumosinski and Harold M. Farrell, Jr

In the development of new foods or in the control of traditional processes, protein functionality plays a paramount role. It has long been theorized that changes in protein structure can alter functionality, but there has been a lack of reliable methodologies for observing protein structural changes in 'real-world' food samples. Here, a technique for determination of the global secondary structure of proteins using Fourier transform infrared (FTIR) spectroscopy in H_2O instead of D_2O is assessed and contrasted with other methodologies for structural determinations. A quantitative procedure is presented for preparing and analysing FTIR spectra of proteins for the determination of their global secondary structural components. As an example, an analysis of the FTIR spectra of egg-white lysozyme is presented and correlated with global secondary structure values calculated from its X-ray crystallographic structure. Other examples of FTIR analyses of food proteins are presented with consideration given to qualitative procedures for more rapid structural analysis of processed samples.

The central dogma of the protein chemist is that primary structure dictates folding and secondary structure, and that in turn a protein's total structure determines its function[1]. A corollary to this concept, for the food protein chemist, is that protein structure determines its functionality in food systems. However, the actual detection of secondary structural changes in food systems has proved to be somewhat problematic. Secondary structural patterns of proteins are characterized by periodic structures such as helices, sheets and extended portions, as well as a variety of turns, loops and disordered coils[1]. In general, secondary protein structure can be determined by several types of instrumental methods such as X-ray crystallography and nuclear magnetic resonance (NMR), circular dichroism (CD) and infrared (IR) spectroscopy.

The traditional method for the precise determination of the static three-dimensional structures of proteins and smaller molecules is X-ray crystallography[2], which allows for elucidation of the structure with a high degree of accuracy. On the other hand, limitations to the utility of X-ray crystallography for the determination of structure–function relationships in proteins include the requirements that the sample be crystalline and that a suitable heavy metal be incorporated without distorting the crystal. Unfortunately, many proteins and other molecules important to the food industry cannot be crystallized at the present time and, of course, the desired functionality for the molecule most likely exists in the solution, gel or colloid state.

Reference to a brand or firm name does not constitute endorsement by the US Department of Agriculture over others of a similar nature not mentioned.

Thomas F. Kumosinski and Harold M. Farrell, Jr are at the Eastern Regional Research Center, ARS, US Department of Agriculture, 600 E. Mermaid Lane, Philadelphia, PA 19118, USA.

Solution secondary structure determination

In contrast to X-ray crystallography, two-dimensional nuclear magnetic resonance (2D NMR) spectroscopy can measure the dynamic solution structure of molecules[3]. This methodology is not as precise as X-ray crystallography, is time consuming and is limited to proteins with ~100 or fewer amino acid residues. Furthermore, this technique requires a high-field NMR spectrometer; usually 500 MHz is needed to increase proton resolution and to obtain well-resolved two-dimensional spectra.

NMR techniques are costly and time consuming, and thus do not provide a routine method of analysis for studying conformational changes of food proteins under a variety of environmental conditions. Researchers in food science as well as biochemistry have turned to other techniques to measure the global secondary structure of proteins. With these methods, a conformational change in a protein can be established although the precise location along the polypeptide chain can, at best, only be inferred. However, such information, obtained in a relatively short period of time, is still invaluable to food scientists and technologists for developing structure–function relationships of food proteins as well as for establishing whether a protein to be used as an ingredient in a food product is in a native or denatured form.

The most widely used technique for estimation of the secondary structure of a protein is circular dichroism (CD) spectroscopy[4]. This technique measures the wavelength dependence in ellipticity (the difference in absorbance between left and right circular polarized light) for the optically active peptide bonds in the far ultraviolet region, mainly 230–185 nm. Three CD bands with either positive or negative maximum ellipticities are produced by peptide bonds for each of the standard conformational states (α-helix, β-sheet and random coil). The combination of nine such positive and negative bands tends to result in ill-defined spectra with low signal-to-noise ratios for proteins containing large amounts of β-sheet and unordered structure. The spectra

observed for residues in an α-helical conformation are much more intense than those for other conformations; thus the method is most reliable for the quantification of helical content. In addition, non-periodic, β-turn structure cannot be distinguished by this methodology. The need to have optically clean solutions (any scattering components will affect the results) and very accurate determinations of the protein concentration complicate the method. However, the need for only small volumes of dilute, aqueous protein solutions is a definite plus.

Fourier transform infrared (FTIR) spectroscopy (see Glossary) experiments, on the other hand, can be performed on samples in any state (solid, solution, gel, colloid, etc.). While FTIR analysis requires high protein concentrations (20–50 mg/ml), only microlitre amounts of the solutions are required.

Previously, D_2O was used for such solution experiments. Now it is possible to perform FTIR analysis of proteins in H_2O instead of D_2O, which offers many advantages. In D_2O, the amide I band is shifted to lower frequencies from under the water peaks at ~1650 cm^{-1}, and unfortunately the amide II band is virtually eliminated. Thus, more information is obtained in H_2O, since the amide I and amide II bands may be concurrently analysed. The vapor spectrum is always properly subtracted, from both the solvent and solution FTIR results, using second-derivative spectra. The high signal of the water peak in D_2O saturates the detector, and a slope as well as a baseline correction must be utilized for proper subtraction of the solvent spectrum from the solution spectrum; this problem is due to the inability to determine the path lengths of the cells accurately. In H_2O a 13 μm cell is used (as opposed to a 75 μm cell in D_2O); thus only a baseline correction is needed, since in H_2O the photomultiplier is not saturated by the intense water peak. Nevertheless, as shown by Dousseau *et al.*[5], careful subtraction of the solvent spectrum from the solution spectrum must be performed when experiments are conducted in H_2O. The subtraction must yield a horizontal line in the 1800–2000 cm^{-1} region, where only water – and not the protein – absorbs infrared radiation. The resulting subtracted spectrum contains an amide II band as well as an amide I band for the protein. Since no slope correction is utilized (as required in the D_2O FTIR experiments), the signal-to-noise ratio remains high (1–1000).

Because of the extremely large signal-to-noise ratio obtained in FTIR, various mathematical techniques can be used to enhance the resolution of the spectra. The resolution of the amide I and amide II bands, which arise from the peptide bonds, can be increased by the use of Fourier transform deconvolution techniques. Individual frequencies within the broad bands can be obtained by calculating the second or even fourth derivatives. The resulting deconvoluted and enhanced spectra can then be fitted to a sum of Gaussian peaks by nonlinear regression analysis to obtain the relative contributions of these individual bands to the total amide I or amide II band. The frequencies of these bands can in turn be correlated with secondary structural assignments using the theoretical calculations of Krimm and Bandekar[6] combined with FTIR spectra obtained for proteins for which three-dimensional X-ray crystal structures are available. The amount of β-turn structure as well as α-helix, 3_{10}-helix, β-sheet or extended strands and unordered structures can be estimated. This methodology is exciting, and its precision as well as its accuracy in the determination of turn structures are now being improved.

Glossary

FTIR spectrophotometer: A spectrophotometer, operating in the infrared region, that uses an interferometer to encode a whole spectral range simultaneously rather than dispersively, one region at a time. A mathematical algorithm, the Fourier transform, is then used to compute a frequency-based vibrational spectrum from the interferogram.

Fourier deconvolution: In the process of transforming the interferogram obtained in the FTIR spectrophotometer, mathematical factors with given limits can be used to increase the resolution of badly overlapped bands with a high signal-to-noise ratio. These functions transform the original Gaussian peaks to ones with greater heights and lower widths at half-height, but that maintain constant area and frequency compared with the original peaks. The process is called deconvolution, and the resulting resolution enhancement can be seen by comparison of Figs 1 and 2 (main plots).

Resolution enhancement factor: A parameter, used in Fourier deconvolution of a spectrum, that is proportional to the desired amount of decrease in the half-width of the peaks in the original spectrum.

Second-derivative spectrum: An idealized infrared absorption band can be described mathematically by a single Gaussian function, but in reality many bands overlap. By mathematically taking the first and then the second derivative over the entire spectrum, each positive Gaussian peak is transformed into a larger negative peak with small positive lobes but with less than half the original width. An example would be the enhancement of the broad 1660 cm^{-1} peak of Fig. 1 in the second-derivative spectrum shown in the inset of Fig. 2.

Pseudo-random deviation plot: Nonlinear regression analysis of a spectrum allows calculation of the deviation of the fitted line from the experimental values at each point. When these residuals (deviations in y) are replotted as a function of x, only short-range positive and negative patterns are acceptable. There should be no long-range describable functions (e.g. sine waves) observed (e.g. see the inset of Fig. 1).

Secondary structural analysis of proteins by FTIR

Overview

With the arrival of commercial FTIR spectrophotometers, methods of analysing IR spectroscopy data to determine the global secondary structure of proteins with a high degree of accuracy and precision have been developed.

In IR spectroscopy the backbone of the polypeptide chain absorbs IR radiation, which excites the vibrational modes of its constituent amide bonds. Two of these vibrational modes are of primary importance to the measurement of protein secondary structure. The first, the amide I vibration, is caused primarily by stretching

of the carbonyl C=O double bonds. The amide II vibration is caused by deformation of the N–H bonds. IR spectroscopy measures the amount of light absorbed due to these vibrations over a range of frequencies of the incident light.

The frequencies at which amide I and amide II bands appear are highly dependent on the secondary structure of the protein, since the chemical environment surrounding the amide linkage affects its motion. However, individual peaks for these vibrational transitions are severely overlapped in FTIR spectra. This overlap needs to be resolved before a complete structural analysis of the protein can be made. Nonlinear regression analysis coupled with Fourier deconvolution techniques have been successfully applied to this problem. An analysis of egg-white lysozyme is given below to demonstrate the methods used.

FTIR analysis of lysozyme

A typical FTIR spectrum with proper solvent and water vapor subtraction of hen's egg-white lysozyme showing both amide I and amide II regions is given as the outer 'envelope' in Fig. 1. This spectrum can be considered to be the sum of a variety of individual bands that arise from specific structural units of the protein, such as α-helix, turns and β-sheets, as well as some side-chain components. Identification of all the components of the spectrum by fitting it directly with an undefined number of Gaussian peaks by nonlinear regression would be a daunting task. To alleviate this dilemma, we first examine the second derivative of the spectrum (Fig. 2; inset) to find the number (n) of component bands and the approximate positions of these peaks.

The next step in the analysis is to enhance the resolution of the original spectrum using a Fourier deconvolution algorithm developed by Kauppinen *et al.*[7] Care must be taken to choose the correct value of the line width and resolution enhancement factors used by this algorithm so that the FTIR spectrum is not over- or under-deconvoluted. (Under-deconvolution is recognized by the absence of a major band indicated by a peak in the second-derivative spectrum; over-deconvolution results in the appearance of large side lobes in the baseline region of the deconvoluted spectrum.) As the deconvolution procedure progresses, analysis of the Fourier-deconvoluted spectrum by nonlinear regression analysis is used in an iterative fashion to help choose the Fourier deconvolution parameters. A model composed of the sum of a series of Gaussian peaks in the range 1700–1500 cm^{-1} is fitted to the deconvoluted spectrum (Fig. 2) by nonlinear regression:

$$A = \sum_{j=1}^{n} h_j[\exp(-(x - x_j)^2 / 2W_j)] \qquad (1)$$

where A is absorbance, W_j is peak width, x_j is frequency in cm^{-1} and h_j is the peak height. The parameters W_j, x_j and h_j for the n peaks are optimized by the regression analysis. A baseline correction is generally not needed after proper background subtraction.

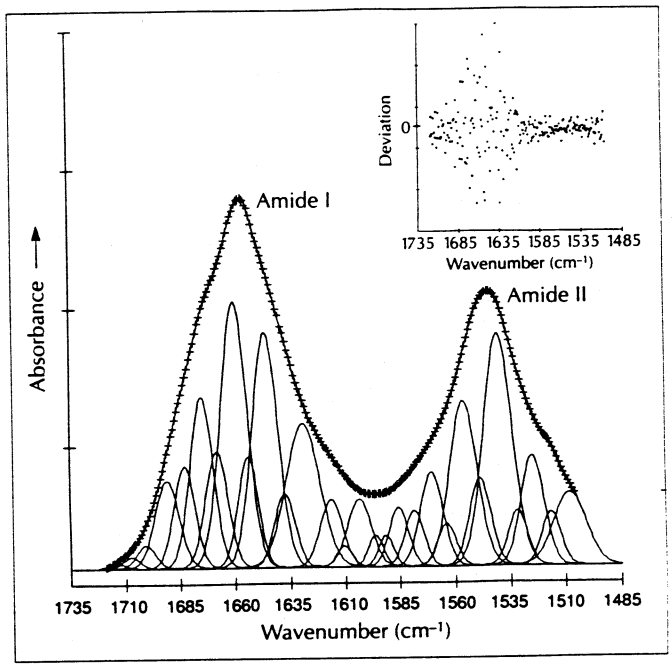

Fig. 1

FTIR spectrum showing amide I and amide II bands of egg-white lysozyme in aqueous solution. Outer 'envelope' (crosses) are the original spectrum. Lines on the outer envelope and individual component peaks underneath are the results of nonlinear regression analysis as described in text. Inset shows a plot of the residuals (deviations) of calculated from experimental absorbances versus frequency (Kumosinski, T.F. and Farrell, H.M., Jr, unpublished).

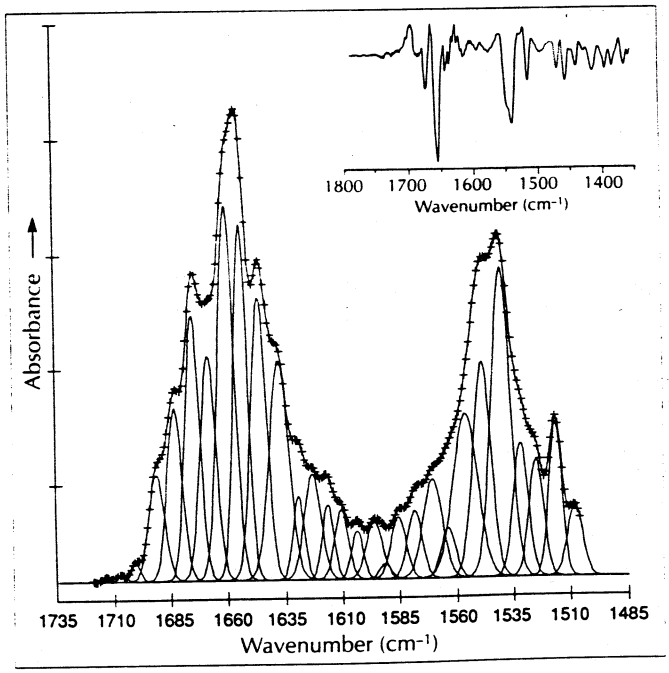

Fig. 2

Fourier deconvolution of the FTIR spectrum of lysozyme shown in Fig. 1. Lines on the outer envelope and individual component peaks underneath were found by regression analysis as described in text. Crosses are experimental data. Inset shows the second derivative of the original spectrum in Fig. 1 (Kumosinski, T.F. and Farrell, H.M., Jr, unpublished).

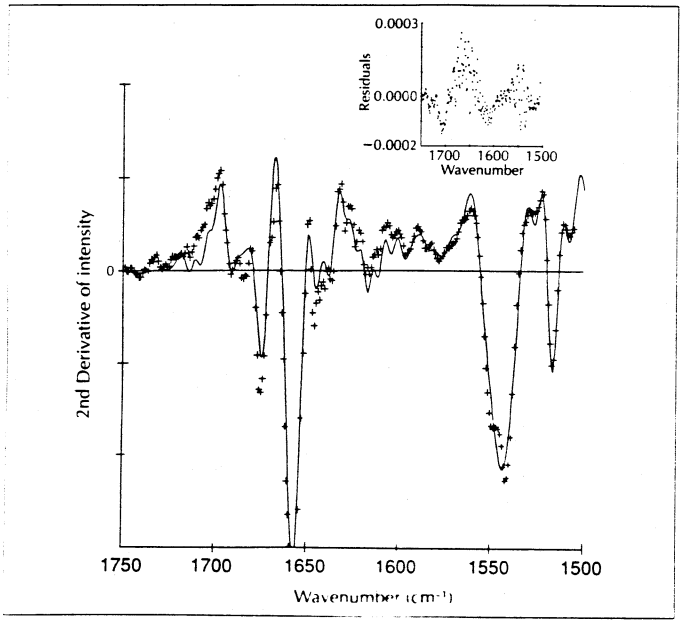

Fig. 3

Second-derivative FTIR spectrum of the amide I and II bands of lysozyme in aqueous solution. Outer envelope crosses are experimental data. The line on the outer envelope and the individual component peaks underneath are the results of final regression analysis as described in text. Insert shows plot of the residuals (deviations) of calculated and experimental second derivative results versus frequency (Kumosinski, T.F. and Farrell, H.M., Jr, unpublished).

Table 1a. Peak assignments in FTIR of lysozyme[a]

Peak assignment	Peak wavenumber (cm^{-1})			
	Helix	Extended	Unordered (loops)	Turns
Amide I	1660	1637	1646	1691
	1655	1629		1683
		1623		1675
				1668
Amide II	1540	1532	1548	1578
		1525		1571
				1564
				1556

Table 1b. Secondary structural analysis in FTIR of lysozyme[b]

Peak assignment	Fraction with secondary structure			
	Helix	Extended	Unordered	Turns
From deconvoluted spectrum:				
Amide I	0.320 ± 0.014	0.204 ± 0.012	0.131 ± 0.003	0.311 ± 0.013
Amide II	0.278 ± 0.012	0.175 ± 0.010	0.183 ± 0.045	0.364 ± 0.101
From original spectrum:				
Amide I	0.266	0.176	0.174	0.384
Amide II	0.323	0.176	0.090	0.411
X-ray structure[c]	0.310	0.155[d]	0.225[e]	0.310

[a] Data taken from Ref. 6
[b] Kumosinski, T.F. and Farrell, H.M., Jr, unpublished
[c] Data taken from Ref. 1
[d] As fraction of β-turns only; does not include all the extended features of the protein
[e] Difference between sum of the other reported fractions and 1

Quantitative criteria to ensure correct deconvolution are:

- correlation of all band assignments with the second-derivative peaks;
- agreement between calculated and experimental baselines;
- a standard deviation of regression that is less than or equal to the experimental noise;
- a successful fit to the original spectrum of the model using fixed frequencies found by fitting the deconvoluted spectrum.

In practice, attainment of these criteria may require several cycles of deconvolution and regression until optimal deconvolution is achieved.

The last of these criteria involves using the results of the regression analysis of the deconvoluted spectrum (Fig. 2) in Eqn 1 to provide the frequencies of the number (n) of bands. These frequencies are then fixed, and a model with the same number of bands and frequencies is then fitted to the original spectrum.

The final fit to the lysozyme FTIR spectrum is shown in Fig. 1 with its 29 component peaks. The inset (Fig. 1) shows that the residuals of the regression are reasonably random, a reliable indication that the model explains the data. Calculated relative areas under the component bands of the original spectrum are in good agreement with those calculated from results of the regression analysis of the Fourier-deconvoluted spectrum.

Further validation of the calculated components of the amide I and II bands can be obtained by mathematical comparison of the second-derivative FTIR spectrum obtained from the original spectrum with a calculated second-derivative spectrum obtained from the model fit. Fractional areas as well as frequencies should be in agreement between calculated values from deconvoluted and fitted spectra and those derived from the original data. The result of such a fit to a second-derivative spectrum of lysozyme is shown in Fig. 3; the curve represents the fitted model and the crosses represent the experimental data. The inset of Fig. 3 shows a reasonable pseudo-random deviation plot whose greatest value (0.0003) falls well within the precision of the instrument. (A slight bias is noted above the 1700 cm^{-1} region, where there are no secondary structural peaks, but this area is dominated by protonated or salt-bound carboxyl group side chains; small biases in other portions of the spectra fall well within the signal-to-noise range of the instrument.) The ability to recalculate the second-derivative plot further establishes the reliability of this methodology for the quantitative resolution of the FTIR spectra of proteins into their individual component bands.

Table 1 shows the assignments of component peaks obtained from the above analysis of lysozyme by reference to previously reported[6] vibrational assignments. From the relative areas under these bands, we can obtain the fractional amounts of the different structural features in the polypeptide chain. Notable bands arising from side-chain components, such as the O–H bond of

tyrosine, which occurs at 1510 cm^{-1}, are also visualized. Replicate values of the fractions due to various polypeptide secondary structures are obtained from amide I and amide II regions. Good agreement between corresponding fractions adds confidence to this analysis. The amide I region gives the best results because the components of the amide II region are inherently more poorly resolved.

The FTIR structural analysis can now be compared with the global secondary structure of lysozyme (Fig. 4) determined by X-ray crystallography. Good agreement is obtained (Table 1), noting that the estimated extended and unordered fractions from X-ray analysis are, by nature, not exact. In this example, fractional amounts of helix and turns from FTIR and X-ray crystallography are quite similar. Such comparisons can be used to determine whether the dynamic structure in water, where the protein maintains a structure more relevant to its biological role, is the same as the structure of the crystalline protein. The same approach is being applied to other proteins for which crystal structures are available. However, many proteins relevant to the food industry have not been crystallized. For these cases, FTIR data can be compared with sequence-based secondary structural predictions. The ultimate goal of this work is to obtain an experimentally based, statistically significant predictor of the secondary structure of proteins that can be related to the amino acid sequence of the polypeptide, and to correlate the FTIR spectra with processing-induced structural changes.

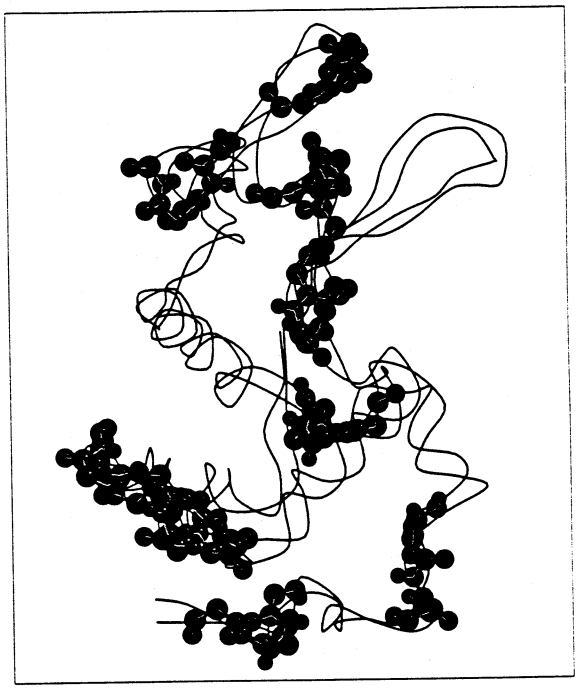

Fig. 4
Molecular modelling representation of the X-ray crystal structure of lysozyme. The double ribbon follows the backbone, while the 'ball-and-stick' atoms represent the backbone structure calculated to be in turn configurations (Kumosinski, T.F. and Farrell, H.M., Jr, unpublished).

Qualitative use of FTIR analysis of proteins and peptides

We now turn our attention to a qualitative method for determining the dominant global secondary structure of a protein and for elucidating whether the protein has undergone any conformational change upon perturbation by environmental factors, such as thermal denaturation. For this procedure the second derivatives of the FTIR spectra, such as in the envelope of Fig. 3 and inset of Fig. 2, are utilized.

It should be noted that the second derivative of a Gaussian peak results in a large negative peak with two small positive lobes on either side. The position of such a negative peak can be used to determine the type of global secondary structure. Its appearance is also an indication that a considerable amount of this structure is present in the protein. For spectra composed of the sum of poorly resolved Gaussian peaks with extremely good precision, such as the FTIR spectra of proteins, second-derivative spectra can be numerically calculated by some algorithm such as the Fourier transform method utilized in the present study.

Figure 5 shows second-derivative FTIR spectra for three globular proteins: lysozyme, myoglobin and β-lactoglobulin. Since the amounts of the various secondary structures for each protein are significantly different, as determined from their X-ray crystallographic structures, all three second-derivative spectra should be markedly different.

Inspection of the amide II region (1530–1570 cm^{-1}) shows very little variation among the three different proteins. The amide I region (1620–1700 cm^{-1}) shows large changes in the number, amount and position of negative peaks for the different proteins, reflecting again the sensitivity of the amide I band over the amide II band.

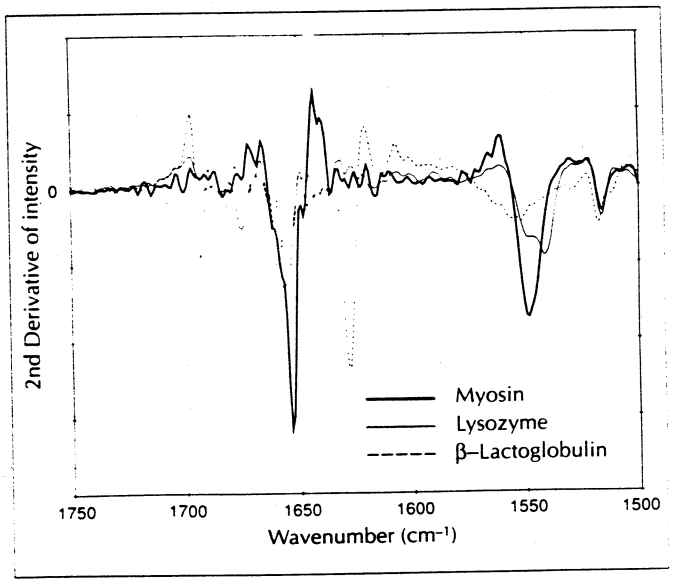

Fig. 5
Calculated second-derivative FTIR spectra of the globular proteins myoglobin, lysozyme and β-lactoglobulin (Kumosinski, T.F. and Farrell, H.M., Jr, unpublished).

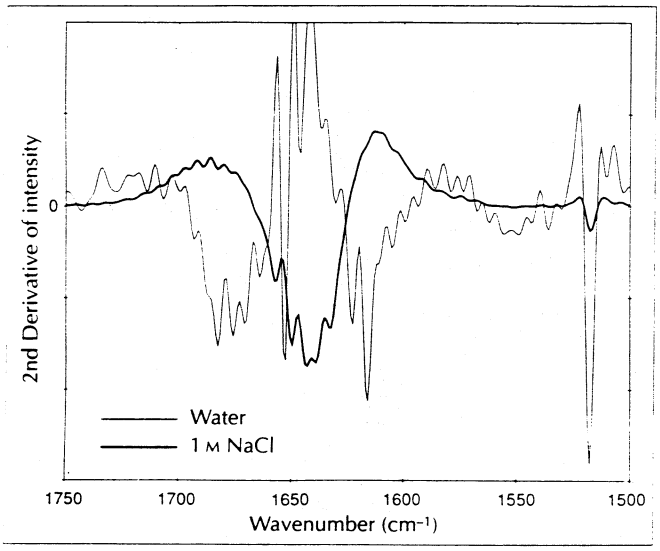

Fig. 6

Calculated second-derivative FTIR spectra of oxytocin in water and 1 M NaCl (Kumosinski, T.F. and Farrell, H.M., Jr, unpublished).

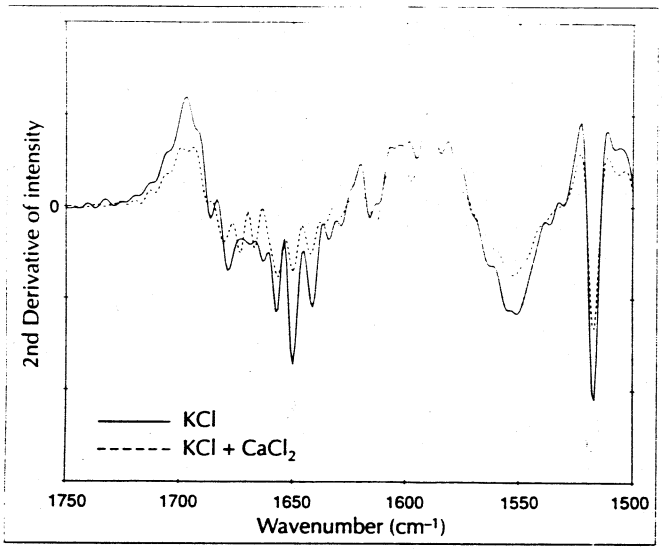

Fig. 7

Calculated second-derivative FTIR spectra of whole casein at 15°C. (———), with added KCl under submicellar conditions; (– – –), with added KCl and $CaCl_2$ under colloidal micellar conditions (Kumosinski, T.F. and Farrell, H.M., Jr, unpublished).

From the X-ray crystal structure, the major secondary structure for myoglobin is α-helix. This is in qualitative agreement with the second-derivative FTIR spectrum of myoglobin in solution since a major negative peak exists at about 1660 cm^{-1}; from the tentative assignments of Krimm and Bandekar[6], this peak is associated with an α-helix conformation (Table 1). It also should be noted that no other negative peaks are observed in the 1620–1700 cm^{-1} region for myoglobin.

The lysozyme second-derivative spectrum, shown as a single line in Fig. 5, has a large negative peak at 1653 cm^{-1} indicating a significant amount of α-helix (but not as much as for myoglobin), and two smaller peaks at 1642 cm^{-1} and 1675 cm^{-1} corresponding to loop or disordered and turn conformations, respectively. These qualitative results are in good agreement with the quantitative global secondary structural analysis from FTIR and X-ray crystallography described above.

The second-derivative FTIR spectrum of β-lactoglobulin is significantly different from the myoglobin and lysozyme spectra. From the X-ray structure, β-lactoglobulin has been shown to be composed predominantly of β-sheets or extended structures and turns with little α-helix and loop conformation. The second-derivative FTIR curve shows two large negative bands at 1695 cm^{-1} and 1628 cm^{-1} for turn and sheet conformations, with almost negligible negative peaks at 1660 cm^{-1} and 1644 cm^{-1}, which are assignments for α-helix and loop conformations, respectively.

This second-derivative analysis is particularly useful for measuring the denaturation of proteins and peptides with added co-solutes. In Fig. 6 a comparison second-derivative FTIR study is shown for oxytocin, a small peptide responsible for the smooth muscle contractions that lead to milk secretion[8]. Here, oxytocin conformational analyses in water and in 1 M NaCl are compared. The crystal structure of oxytocin shows that the peptide is composed of turn and some sheet conformation. The spectrum of oxytocin in water contains two main negative peaks centred at 1623 cm^{-1} and 1675 cm^{-1} and assigned as sheet and turns, respectively. Upon the addition of 1 M NaCl, these peaks disappear and large negative peaks are obtained only at 1644 cm^{-1}, corresponding to loop structures. Hence, the internal hydrogen bonds of oxytocin that are responsible for its sheet and turn structures are disrupted by 1 M NaCl, and a loop or denatured structure instead predominates.

Finally, this method can be used to compare the solution form of the protein with its salt-induced colloidal state. For this purpose, we have compared whole bovine casein in KCl under submicellar conditions (radius: ~80 Å) with casein in $CaCl_2$, whereby the protein aggregates to form a colloidal particle (radius: ~700 Å)[9]. Figure 7 shows that little or no conformational change occurs for whole casein at 15°C upon the formation of a colloidal micelle with added $CaCl_2$. Only minor differences are observed between the two forms in the second-derivative FTIR spectra, in spite of the light scattering that accompanies colloid formation. Such a comparative study could not be performed previously because CD spectroscopy, for example, is greatly affected by light scattering from large particles. The colloidal casein micelle CD spectrum would be highly degraded due to such extensive light-scattering effects.

Concluding remarks

FTIR spectroscopy of proteins in H_2O can be an important tool for developing structure–function relationships in food science as well as in biological systems. In particular, changes in the global secondary structure of proteins can be correlated with changes in environmental conditions such as temperature, pH or added co-solutes. The funtionality of these protein systems can then be determined under the same conditions. 'Real-world' samples exhibiting light scattering can also be evaluated.

Quantitative methods for the determination of protein secondary structure can easily be used to resolve the ill-defined amide I and amide II bands into their individual structure component bands, due to the inordinately good signal-to-noise ratio given by the method. We have chosen Fourier deconvolution and the calculation of second-derivative spectra by Fourier transform techniques in conjunction with nonlinear regression analysis to analyse these spectra. (Software for these computations can be obtained by writing to Dr William Damart, Eastern Regional Research Center, US Department of Agriculture, Wyndmoor, PA 19118, USA.) The individual investigator may, however, use other methodologies than those presented here. What is necessary is that the method employed leads to consistent results with good precision.

A qualitative procedure for estimating major secondary structural features of proteins by the determination of second-derivative FTIR spectra of proteins in H_2O, such as the example given above, easily allows the food scientist to show whether a major conformational change can occur as a given food system under investigation is perturbed. A future use of such a qualitative approach may be established by the food industry in the field of quality control during the processing of food products, or to determine whether a raw protein ingredient such as whey protein isolate or concentrate, sodium caseinate, soy isolate, etc. will be of adequate quality to create a high-quality food product. It is hoped that in the future all companies selling such raw materials will provide their industrial customers with a second-derivative FTIR spectrum with each batch of protein.

References

1 Fasman, G.D., ed. (1989) *Prediction of Protein Structure and the Principles of Protein Conformation*, Plenum Press

2 Cantor, C.R. and Schimmel, P.R. (1980) *Biophysical Chemistry Part II: Techniques for the Study of Biological Structure and Function*, pp. 687–791, W.H. Freeman

3 Wüthrich, K. (1989) *Science* 243, 45–50

4 Yang, J.T., Wu, C-S.C. and Martinez, H.M. (1986) *Methods Enzymol.* 130, 208–269

5 Dousseau, F., Therrien, M. and Pézolet, M. (1989) *Appl. Spectrosc.* 43, 538–542

6 Krimm, S. and Bandekar, J. (1986) *Adv. Protein Chem.* 38, 181–364

7 Kauppinen, J.K., Moffatt, D.J., Mantsch, H.H. and Cameron, D.G. (1981) *Appl. Spectrosc.* 35, 271–276

8 Robinson, I.C.A.F. (1986) *Curr. Top. Neuroendocrinol.* 6, 153–172

9 Kumosinski, T.F. and Farrell, H.M., Jr (1991) *J. Protein Chem.* 10, 3–16